Organic−Inorganic Hybrids Based on Polyoxometalates. 6.[1] Syntheses, Structure, and Reactivity of the Bis(*tert*-butylsilyl)decatungstophosphate $[(\gamma\text{-}PW_{10}O_{36})(t\text{-}BuSiOH)_2]^{3-}$

Agnès Mazeaud, Yves Dromzee, and René Thouvenot*

Laboratoire de Chimie Inorganique et Matériaux Moléculaires, ESA 7071, Université Pierre et Marie Curie, case courrier 42, 4 Place Jussieu, 75252 Paris Cedex 05, France

Received May 2, 2000

Bis(*tert*-butylsilyl)decatungstophosphate $(n\text{-}Bu_4N)_3[(\gamma\text{-}PW_{10}O_{36})(t\text{-}BuSiOH)_2]$ (**1**) has been synthesized through phase-transfer conditions, by reaction of $t\text{-}BuSiCl_3$ with $Cs_7[(\gamma\text{-}PW_{10}O_{36})]\cdot xH_2O$. This new hybrid anion has been characterized by elemental analysis, X-ray crystallography, multinuclear solution and solid-state NMR, and infrared spectroscopy. Crystals of **1** are monoclinic, space group *C*2/*c*, with lattice constants $a = 44.762(10)$ Å, $b = 19.032(4)$ Å, $c = 22.079(8)$ Å, $\beta = 98.9(2)°$, and $Z = 8$. Anion **1** has nominal C_s symmetry and displays an "open structure" with two *t*-BuSiOH groups anchored to the $(\gamma\text{-}PW_{10}O_{36})$ framework. The two *t*-BuSiOH units are nonequivalent as confirmed by ^{29}Si CP-MAS NMR and by diffuse reflection infrared spectroscopy. The two OH groups are linked through one H-bond ($d_{O-O} = 2.63$ Å). According to ^{29}Si and ^{183}W NMR, **1** adopts a more symmetrical conformation (C_{2v}) in solution. Anion **1** reacts cleanly in homogeneous conditions with Me_2SiCl_2 to yield $(n\text{-}Bu_4N)_3[(\gamma\text{-}PW_{10}O_{36})(t\text{-}BuSiO)_2(SiMe_2)]$ (**2**). The structure of **2** has been inferred from multinuclear NMR and infrared spectroscopy. The hybrid "closed-structure" anion **2** consists of the $(\gamma\text{-}PW_{10}O_{36})$ framework on which is grafted a heterosilylated network composed of a capping fragment, $Si(CH_3)_2$, linked to the *t*-BuSi groups through two siloxane bridges.

Introduction

During the past few decades, interest for polyoxometalates (POMs) has been continuously growing, supported by the improvement of technical structural analysis, such as X-ray diffraction and NMR, IR, and Raman spectroscopies. But they have also received much attention because of practical applications due to the versatility of their properties. They have found applications in medicine, biology, catalysis, material science, etc.[2]

Particularly, heteropolyoxometalates with an organic group anchored to their backbone are interesting precursors for hybrid organic−inorganic materials. For example, organosilicon derivatives of undecatungstopolyoxometalates have been studied for a long time,[3,4] but few compounds have been synthesized. Earlier work demonstrated that a $(RSi)_2O^{4+}$ unit may replace a WO_4^{4+} unit to yield $[SiW_{11}O_{39}(SiR)_2O]^{4-}$. Anti-HIV1 activity of this polyanion has been tested,[5] and it has also proved to be an efficient precursor for synthesis of hybrid polymers.[6]

For several years, we have been investigating the reactivity of trichlorosilanes, under phase-transfer conditions, with various polyvacant heteropolyoxotungstates.[7] Previous results have shown that closed or open structures are formed. Following this work, we describe here the synthesis and characterization of two new organosilyl derivatives, based on the $\gamma\text{-}PW_{10}$ structure.

Experimental Section

Synthesis. Cesium γ-decatungstophosphate $(Cs_7[\gamma\text{-}PW_{10}O_{36}]\cdot xH_2O)$ was synthesized following the published method,[8] and its purity was checked by infrared spectroscopy. *tert*-Butyltrichlorosilane and dimethyldichlorosilane were purchased from Aldrich and were used as supplied.

$(n\text{-}Bu_4N)_3[(\gamma\text{-}PW_{10}O_{36})(t\text{-}BuSiOH)_2]$ (1). To a well-stirred suspension of 5 g of $Cs_7[\gamma\text{-}PW_{10}O_{36}]\cdot xH_2O$ (1.4 mmol) in 50 mL of freshly distilled acetonitrile were added, under argon, 2.5 g of solid $n\text{-}Bu_4NBr$ (5.6 mmol) and 0.81 g of $t\text{-}BuSiCl_3$ (4.2 mmol). The mixture was stirred overnight at 0 °C. The solid (essentially CsBr + CsCl) was separated by filtration and washed with about 10 mL of acetonitrile. Then, the yellow filtrate was allowed to stand at room temperature, in an open vessel, and after 1 day, well-shaped yellow crystals (3 g, yield 60%), suitable for X-ray analysis, were obtained. Anal. Calcd for $C_{56}H_{128}N_3O_{38}PSi_2W_{10}$: C, 19.92; H, 3.82; N, 1.24; P, 0.92; Si, 1.66; W, 54.44. Found: C, 20.07; H, 3.52; N, 1.32; P, 1.21; Si, 1.78; W, 53.28. ^1H NMR: δ 1.0 (s, $(CH_3)_3C$, 18H), 5.0 (s, OH, 2H). $^{13}C\{^1H\}$ NMR: δ 18.9 (s, $(CH_3)_3C-Si$), 26.6 (s, $(CH_3)_3C-Si$). ^{31}P NMR: δ −14.7. ^{29}Si NMR: δ −44.6 ($^3J_{SiH} = 6.6$ Hz, $^2J_{WSi} = 9.5$ Hz). For ^{183}W NMR data, see Table 4.

$(n\text{-}Bu_4N)_3[(\gamma\text{-}PW_{10}O_{36})(t\text{-}BuSiO)_2(SiMe_2)]$ (2). A 2 g sample of **1** (0.6 mmol) was dissolved in 5 mL of deaerated DMF. Under argon, 3 equiv of Me_2SiCl_2 (0.22 mL, 1.8 mmol) was added. The solution was stirred for 48 h at room temperature, and then set aside. After a few days, 1.5 g of white crystals (75%) was obtained. Anal. Calcd for

* To whom correspondence should be addressed. E-mail: rth@ccr.jussieu.fr. Fax: 33 1 44 27 38 41.

(1) Part 5: Mayer, C. M.; Herson, P.; Thouvenot, R. *Inorg. Chem.* **1999**, *38*, 6152.
(2) (a) Pope, M. T. *Heteropoly and Isopoly Oxometalates*; Springer-Verlag: Berlin, 1983. (b) Pope, M. T. Isopoly and Heteropolyanions. In *Comprehensive Coordination Chemistry*; Wilkinson, G., Gillard, R. D., McCleverty, J. A., Eds.; Pergamon Press: Oxford, 1987; p 1023. (c) Pope, M. T. *Prog. Inorg. Chem.* **1991**, *39*, 181. (d) Pope, M. T.; Müller, A. *Angew. Chem., Int. Ed. Engl.* **1991**, *30*, 34. (e) *Polyoxometalates: From Platonic Solids to Ant-Retroviral Activity*; Pope, M. T., Müller, A., Eds.; Kluwer Academic Publishers: Dordrecht, The Netherlands, 1994.
(3) Knoth, W. H. *J. Am. Chem. Soc.* **1979**, *101*, 759.
(4) Judeinstein, P.; Deprun, C.; Nadjo, L. *J. Chem. Soc., Dalton Trans.* **1991**, 1991.
(5) Weeks, M. S.; Hill, C. L.; Schinazi, *J. Med. Chem.* **1992**, *35*, 1216.
(6) Judeinstein, P. *Chem. Mater.* **1992**, *4*, 4.
(7) (a) Ammari, N.; Hervé, G.; Thouvenot, R. *New J. Chem.* **1991**, *15*, 607. (b) Mazeaud, A.; Ammari, N.; Robert, F.; Thouvenot, R. *Angew. Chem., Int. Ed. Engl.* **1996**, *35*, 1961.
(8) (a) Knoth, W. H.; Harlow, R. L. *J. Am. Chem. Soc.* **1981**, *103*, 1865. (b) Domaille, P. J. *Inorg. Synth.* **1990**, *27*, 96.

10.1021/ic0004784 CCC: $19.00
Published on Web 09/27/2000

Table 1. Crystallographic Data for $(n\text{-Bu}_4\text{N})_3[(\gamma\text{-PW}_{10}\text{O}_{36})(t\text{-BuSiOH})_2]$ (**1**)

empirical formula	$C_{56}H_{128}O_{38}N_3Si_2PW_{10}$	V, Å^3	18 582(9)
fw	3377.27	Z	8
space groupe	$C2/c$	λ, Å	0.710 69
T, °C	25	$\rho_{calcd.}$, g·cm^{-3}	2.41
a, Å	44.762(10)	μ, cm^{-1}	127.13
b, Å	19.032(4)	R^a	0.079
c, Å	22.079(8)	$R_w{}^b$	0.091
α, deg	90		
β, deg	98.9(2)		
γ, deg	90		

^{a} $R = \sum||F_o| - |F_c||/\sum|F_o|$. ^{b} $R_w = [\sum w(|F_o| - |F_c|)^2/\sum wF_o^2]^{1/2}$.

$C_{58}H_{132}N_3O_{38}PSi_3W_{10}$: C, 20.29; H, 3.88; N, 1.22; P, 0.98; Si, 2.45; W, 53.55. Found: C, 19.51; H, 3.81; N, 1.21; P, 1.40; Si, 2.10; W, 53.53. ^{1}H NMR: δ 1.0 (s, $(CH_3)_3C$, 18H), 0.15 (s, $(CH_3)_2-Si$, 6H); $^{13}C\{^1H\}$ NMR: δ 0.5 (s, $(CH_3)_2-Si$), 18.9 (s, $(CH_3)_3C-Si$), 26.2 (s, $(CH_3)_3C-Si$). ^{31}P NMR: δ − 14.4. ^{29}Si NMR: δ − 20.3 (1Si, $^2J_{SiH}$ = 7.4 Hz), − 52.9 (2Si, $^3J_{SiH}$ = 6.7 Hz, $^2J_{WSi}$ = 10.5 Hz). For ^{183}W NMR data, see Table 4.

Physical Measurements. Elemental analyses were performed by the "Service central de microanalyse du CNRS", Vernaison, France. The transmission infrared spectra were recorded on an IRFT spectrometer Bio-Rad FTS 165 on KBr pellets. The diffuse reflection spectrum of **1** diluted in KBr was obtained using the DRIFT Digilab accessory, and the data are presented in Kubelka−Munk units, $(1 - R)^2/2R$, where R represents the ratio of the sample reflectance with respect to pure KBr reflectance. ^{29}Si solution spectra were obtained on a Bruker AM500 spectrometer, operating at 99.35 MHz, in 10 mm o.d. tubes, either in undecoupled one-pulse mode for quantitative purposes, or using coupled or decoupled INEPT sequences for improved signal/noise ratio. All other solution spectra were obtained on a Bruker AC300 spectrometer at 300.13, 75.47, and 121.5 MHz for ^{1}H, ^{13}C, and ^{31}P, respectively, in 5 mm o.d. tubes and at 12.5 MHz for ^{183}W in 10 mm o.d. tubes. Chemical shifts are reported according to IUPAC convention with respect to internal CHD_2CN or CHD_2CD_3SO for ^{1}H, internal CD_3CN or DMSO-d_6 for ^{13}C, external tetramethysilane for ^{29}Si, and external 85% H_3PO_4 for ^{31}P. ^{183}W chemical shifts are measured with respect to external 2 M Na_2WO_4 solution in D_2O, using saturated dodecatungstosilicic acid (D_2O solution) as the secondary standard ($\delta = -103.8$ ppm). All NMR experiments were done in acetone-d_6 or DMSO-d_6 for ^{13}C and ^{1}H and in mixed solvent DMF/acetone-d_6 (80/20, v/v) for ^{29}Si, ^{31}P, and ^{183}W. Solid-state CP-MAS ^{29}Si spectra were recorded on a Bruker MSL400 spectrometer operating at 79.5 MHz, with powdered samples packed in a 7 mm diameter double-bearing rotor.

Crystallography. Data for $(n\text{-Bu}_4\text{N})_3$ **1** were collected at room temperature with a $\theta-2\theta$ technique on a MACH3 Enraf-Nonius diffractometer using graphite-monochromated Mo Kα radiation (λ = 0.710 69 Å). The crystal was mounted on a glass fiber and sealed with epoxy cement. Unit cell dimensions were obtained from least-squares refinement of the setting angles of 25 automatically centered reflections. References were periodically monitored for intensity and orientation control: they showed a decay of about 40% over the entire course of data collection (4 days), likely due to solvent loss. Corrections for polarization and Lorentz effects were applied, and absorption was corrected by DIFABS. Computations were performed by using the CRYSTALS program.[9] W atom coordinates were obtained by the direct method (SHELXS-86),[10] and coordinates of the other atoms were determinated using successive difference Fourier maps. W, P, and Si atoms were refined anisotropically; all other atoms were refined isotropically. Hydrogen atoms were not included. Crystal data and structure refinement parameters are listed in Table 1; selected bond lengths are given in Table 2.

Table 2. Selected Bond Lengths and Averages (Å) for $(n\text{-Bu}_4\text{N})_3[(\gamma\text{-PW}_{10}\text{O}_{36})(t\text{-BuSiOH})_2]$ (**1**)

	bond length (Å)	av		bond length (Å)	av
W=O	1.60(4)−1.72(5)	1.68	Si−O(W)	1.62(3)−1.70(4)	1.65
W−O(W)	1.74(4)−2.11(4)	1.90	Si−O(H)	1.60(5)−1.76(6)	1.68
W−O(Si)	1.85(4)−1.89(3)	1.87	Si−C	1.94(7)−1.97(8)	1.95
W−O(P)	2.31(4)−2.47(5)	2.37	C−C	1.4(1)−1.7(2)	1.50
P−O	1.55(4)−1.61(4)	1.58			

Results and Discussion

Synthesis. The divacant anions $[\gamma\text{-SiW}_{10}\text{O}_{36}]^{8-}$ [11] and $[\gamma\text{-PW}_{10}\text{O}_{36}]^{7-}$ [8] are lacunary derivatives of the γ-isomers of the Keggin structure. Numerous addition derivatives of $[\gamma\text{-SiW}_{10}\text{O}_{36}]^{8-}$ have been described in the past few years,[12−14] but little has been done with $[\gamma\text{-PW}_{10}\text{O}_{36}]^{7-}$, likely because it is unstable in aqueous solution.[15,16] Even its saturated derivative $[\gamma\text{-PV}_2\text{W}_{10}\text{O}_{36}]^{5-}$ isomerizes in aqueous solution. However, the stable saturated hybrid derivative $[(\gamma\text{-PW}_{10}\text{O}_{36})(t\text{-BuSiOH})_2]^{3-}$ is easily prepared from the reaction of $Cs_7[\gamma\text{-PW}_{10}\text{O}_{36}]\cdot x\text{H}_2\text{O}$ with t-$BuSiCl_3$. As for the preparation of organosilyl derivatives of trivacant polytungstates, the reaction proceeds under phase-transfer conditions with n-Bu_4N^+ acting as the transfer agent.[7]

$$[\gamma\text{-PW}_{10}\text{O}_{36}]^{7-} + 2t\text{-BuSiCl}_3 + 2\text{H}_2\text{O} \rightarrow [(\gamma\text{-PW}_{10}\text{O}_{36})(t\text{-BuSiOH})_2]^{3-} + 2\text{HCl} + 4\text{Cl}^-$$
1

The water required for hydrolysis of the chlorosilane is furnished by the hydrated polytungstate itself and is delivered progressively in the reaction mixture. **1** is soluble as n-Bu_4N^+ salt in polar organic solvents such as acetonitrile, dimethylformamide, and dimethyl sulfoxide, from which it may be recrystallized. It has been characterized by X-ray crystallography. All NMR data confirm that the structure of the anion is maintained in solution. Like other "open-structure" POMs i.e., $[(\text{A-PW}_9\text{O}_{34})(t\text{-BuSiOH})_3]^{3-}$ and $[(\text{B-As}^{III}\text{W}_9\text{O}_{33})(t\text{-BuSiOH})_3]^{3-}$,[7] this new anion reacts with organochlorosilanes in homogeneous conditions: thus, $[(\gamma\text{-PW}_{10}\text{O}_{36})(t\text{-BuSiOH})_2]^{3-}$ reacts cleanly, as shown by ^{31}P NMR, with Me_2SiCl_2 in DMF to yield $[(\gamma\text{-PW}_{10}\text{O}_{36})(t\text{-BuSiO})_2(\text{SiMe}_2)]^{3-}$ (**2**):

$$[(\gamma\text{-PW}_{10}\text{O}_{36})(t\text{-BuSiOH})_2]^{3-} + \text{Me}_2\text{SiCl}_2 \rightarrow [(\gamma\text{-PW}_{10}\text{O}_{36})(t\text{-BuSiO})_2(\text{SiMe}_2)]^{3-} + 2\text{HCl}$$
1 **2**

The molecular structure of **2** has been inferred from spectroscopic data by comparison with those of **1**. Like **1**, **2** is stable in air as well as in solution.

Crystal Structure. The molecular structure of anion $[(\gamma\text{-PW}_{10}\text{O}_{36})(t\text{-BuSiOH})_2]^{3-}$ is shown in Figure 1. This hybrid anion is built up from a polyoxotungstophosphate framework

(9) Watkin, D. J.; Carruthers, J. R.; Betteridge, P. W. *CRYSTALS, An Advanced Crystallographic Computer Program*; Chemical Crystallographics Laboratory: Oxford, U.K., 1989.
(10) Sheldrick, G. M. *SHELXS-86, Program for Crystal Structure Solution*; University of Göttingen: Göttingen, Germany, 1986.
(11) Canny, J.; Tézé, A.; Thouvenot, R.; Hervé, G. *Inorg. Chem.* **1986**, *27*, 85.
(12) (a) Wassermann, K.; Palm, R.; Lunk, H. J.; Fuchs, J.; Steinfeld, N.; Stösser, R. *Inorg. Chem.* **1995**, *34*, 5029. (b) Wassermann, K.; Lunk, H. J.; Palm, R.; Fuchs, J.; Steinfeld, N.; Stösser, R.; Pope, M. T. *Inorg. Chem.* **1996**, *35*, 3273.
(13) Cadot, E.; Béreau, V.; Marg, B.; Halut, S.; Sécheresse, F. *Inorg. Chem.* **1996**, *35*, 3099.
(14) (a) Zhang, X.; O'Connor, C. J.; Jameson, G. B.; Pope, M. T. *Inorg. Chem.* **1996**, *35*, 30. (b) Xin, F.; Pope, M. T. *Inorg. Chem.* **1996**, *35*, 5695.
(15) Domaille, P. J.; Harlow, R. L. *J. Am. Chem. Soc.* **1986**, *108*, 2108.
(16) Cadot, E.; Béreau, V.; Sécheresse, F. *Inorg. Chim. Acta* **1996**, *252*, 101.

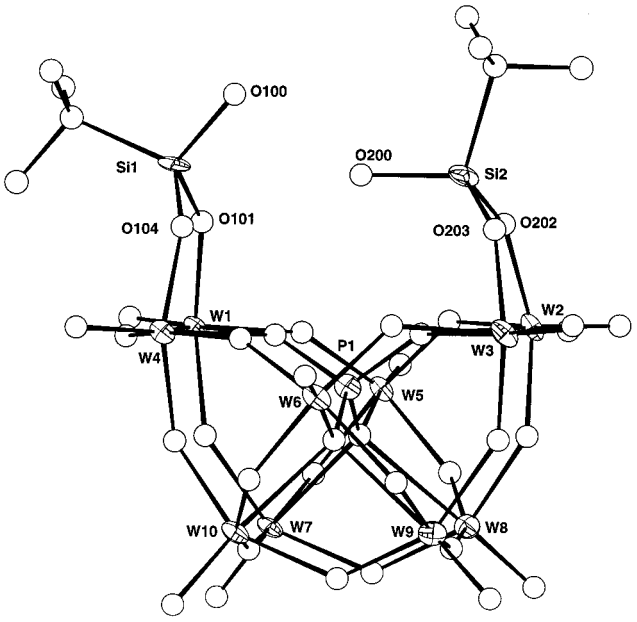

Figure 1. Cameron representation of anion $[(\gamma\text{-}PW_{10}O_{36})(t\text{-}BuSiOH)_2]^{3-}$ (**1**).

Chart 1. Local Environment of the Si Atoms in **1**

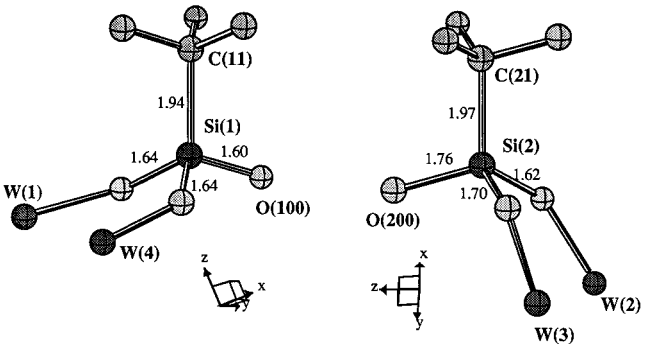

on which are linked two *t*-BuSiOH groups. Each organosilyl group is attached to a dimetallic unit of the polytungstate backbone through two W−O−Si bridges. The polytungstate framework keeps the geometry of the parent divacant anion γ-PW_{10}, which corresponds to an approximate C_{2v} symmetry, but the whole anion presents a lower virtual symmetry (C_s), according to a noncrystallographic mirror plane which contains the two Si atoms.

For the PW_{10} moiety, the interatomic distances and bond angles are in the classical range observed in saturated polyoxotungstate species (Table 2). In particular the W−O bonds in the Si−O−W bridge as well as the trans W−O bonds are all characteristic of normal single bonds (1.85 to 1.89 Å), whereas in the lacunary precursor $[\gamma\text{-}PW_{10}O_{36}]^{7-}$ they are respectively significantly shorter (1.72−1.75 Å for "terminal" O atoms) and larger (2.15−2.16 Å) because of the trans influence.

The silicon atoms are linked to one carbon atom of the *t*-Bu group (d_{Si-C} = 1.94−1.97 Å) and to two oxygen atoms of the POM unit (d_{Si-O} = 1.62−1.70 Å); the tetrahedral environment of the silicon atom is completed by an OH group which results from the hydrolysis of the Si−Cl bond. For Si(1) the Si−O(H) bond is relatively short (1.60(6) Å), but it is slightly larger (1.76(6) Å) for Si(2). This results in a local environment more regular for Si(1) with three nearly equal Si−O bonds (pseudo-C_{3v} symmetry) than for Si(2) (Chart 1). The differences in Si−O(H) bonds can be interpreted by considering the O−O distance between the two silanol groups (d_{O-O} = 2.63 Å). Actually this

Chart 2. Intramolecular H-Bond between the Silanol Groups

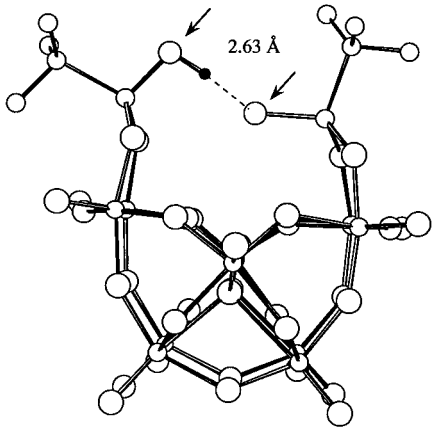

relatively short distance suggests the existence of an intramolecular hydrogen bond between Si(1)−OH acting as hydrogen bond donor and Si(2)−OH acting as an acceptor (Chart 2).[17]

Another interesting feature of this structure is the relative orientation of the two independent *t*-BuSiOH units: actually for Si(2), the Si−O bond is nearly parallel to the plane defined by the four oxygen atoms [O(101), O(104), O(202), O(203)], whereas for Si(1), the Si−O bond is oblique with respect to this plane. Thus, the dihedral angle between the planes [(Si(2), O(202), O(203)] and [W(2), W(3), O(202), O(203)] has an internal concavity with an angle of 155.7°, whereas with nearly the same angle (159.73°), the dihedron formed by planes [(Si(1), O(101), O(104)] and [W(1), W(4), O(101), O(104)] presents an external concavity (Figure 1).

Infrared Spectroscopy. Infrared spectra of **1** and **2** are shown in Figure 2, and the characteristic vibrational data are given in Table 3. The infrared spectrum of **1**, in the 1200−250 cm^{-1} region, is very similar to that observed for the parent derivative $Cs_7[\gamma\text{-}PW_{10}O_{36}]\cdot xH_2O$.[8] In the stretching vibration part, a shift to higher wavenumbers indicates stabilization of the POM framework, which becomes saturated by grafting of the organosilyl groups.[18] For both anions a complex pattern is observed in the 420−250 cm^{-1} region, which is the most sensitive to the type of isomer.[19] Actually the high number of vibrational bands and their relative intensities are characteristic of the γ-isomer.[11,13,16,20] Moreover, the three well-resolved bands at 1117, 1066, and 1041 cm^{-1} assigned to the ν_{P-O} stretching modes are evidence[15,16] of the low symmetry of the central PO_4 tetrahedron, at the most C_{2v}.[21] The diffuse reflection spectrum of **1** confirms an intramolecular hydrogen bond between the two silanol groups: actually two bands are observed in the 3000−4000 cm^{-1} region, characteristic of ν_{OH} stretching vibrations. The broad low-frequency signal at 3395 cm^{-1} could be assigned to the OH vibrator acting as H-bond donor, whereas the narrow band at higher frequency (3564 cm^{-1}) corresponds to a "free" OH vibrator.[22]

(17) Hamilton, W. C.; Ibers, J. A. *Hydrogen Bonding in Solids*; W. A. Benjamin, Inc.: New York, 1968.
(18) Rocchiccioli-Deltcheff, C.; Thouvenot, R. *C. R. Acad. Sci., Ser. C* **1974**, *278*, 857.
(19) Thouvenot, R.; Fournier, M.; Franck, R.; Rocchiccioli-Deltcheff, C. *Inorg. Chem.* **1984**, *23*, 598.
(20) Tézé, A.; Canny, J.; Gurban, L.; Thouvenot, R.; Hervé, G. *Inorg. Chem.* **1996**, *35*, 1001.
(21) Rocchiccioli-Deltcheff, C.; Thouvenot, R. *Spectrosc. Lett.* **1979**, *12*, 127.
(22) Vinogradov, S. N.; Linnell, R. H. *Hydrogen Bonding*; Van Norstrand Reinhold Co.: New York, 1971.

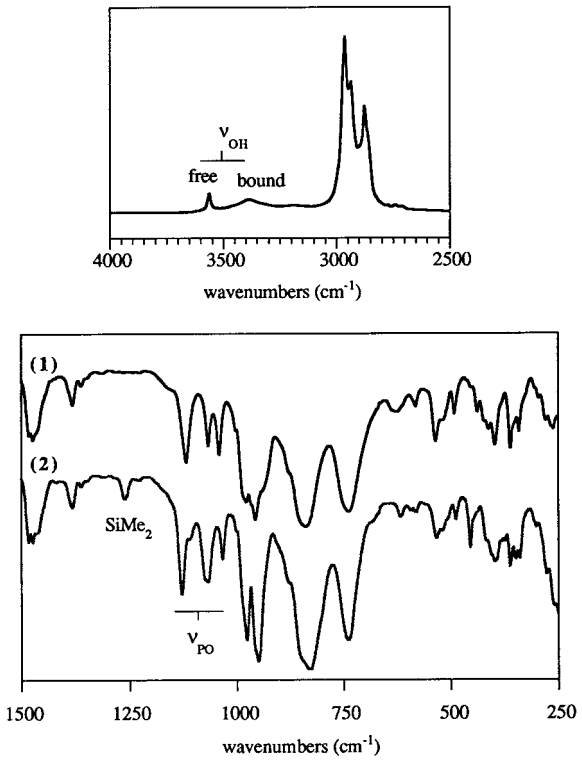

Figure 2. Infrared spectra of $(n\text{-Bu}_4\text{N})_3[(\gamma\text{-PW}_{10}\text{O}_{36})(t\text{-BuSiOH})_2]$ (**1**) and $(n\text{-Bu}_4\text{N})_3[(\gamma\text{-PW}_{10}\text{O}_{36})(t\text{-BuSiO})_2(\text{SiMe}_2)]$ (**2**): (a, bottom) transmission spectra of **1** and **2**; (b, top) reflectance spectrum of **1**.

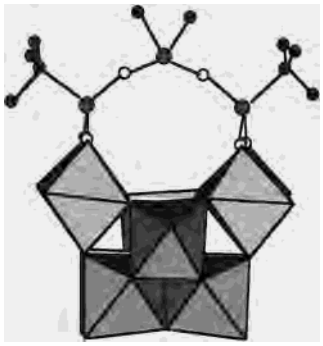

Figure 3. Postulated structure of the anion $[(\gamma\text{-PW}_{10}\text{O}_{36})(t\text{-BuSiO})_2(=\text{SiMe}_2)]^{3-}$ (**2**).

Table 3. Infrared Data and Assignments for $(n\text{-Bu}_4\text{N})_3[(\gamma\text{-PW}_{10}\text{O}_{36})(t\text{-BuSiOH})_2]$ (**1**) and $(n\text{-Bu}_4\text{N})_3[(\gamma\text{-PW}_{10}\text{O}_{36})(t\text{-BuSiO})_2(\text{SiMe}_2)]$ (**2**)

	ν_{OH}	ν_{Si-R}	$\nu_{Si-O-Si}$	ν_{P-O}	$\nu_{W=O}$	ν_{W-O-W}
1	3564 3395			1117 s 1066 s 1041 m	978 s 957 vs 940 s	839 vs 738 vs
2		1260 m	1107 sh	1128 s 1067/1074 1033 m	977 s 949 vs	831 vs 738 vs

For the polyoxometalate part the spectrum of **2** is very similar to that of **1**. The ν_{OH} vibrations observed for **1** are replaced by two bands at 1260 and 1107 (shoulder) cm^{-1}, characteristic of the presence of the $Si(CH_3)_2$ fragment, linked to the *t*-BuSi groups via two siloxane bridges, in accordance with the postulated structure represented in Figure 3.

^{31}P NMR Spectroscopy. ^{31}P spectra of compounds **1** and **2** show a single peak at −14.7 and −14.4 ppm, respectively. These chemical shifts compare well with that of the saturated Keggin anion $[\alpha\text{-PW}_{12}\text{O}_{40}]^{3-}$ ($\delta = -14.55$ ppm).[8b] As for organosilyl

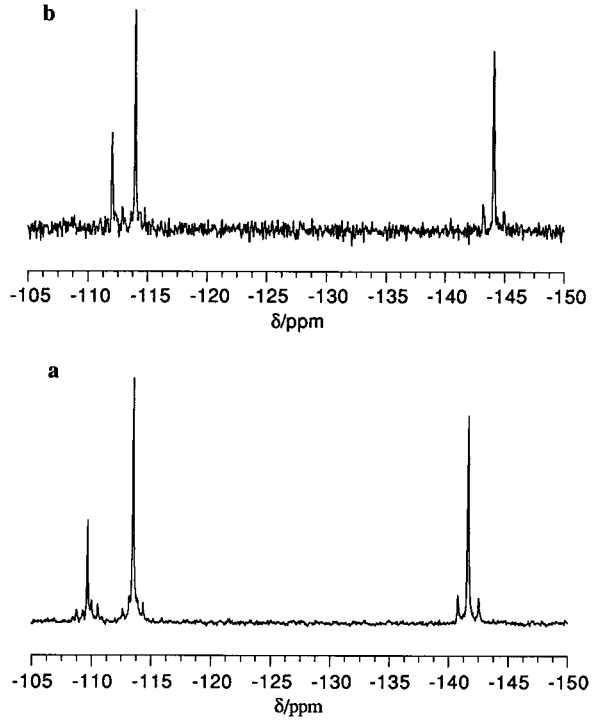

Figure 4. ^{31}P-decoupled ^{183}W spectra of (a) $(n\text{-Bu}_4\text{N})_3[(\gamma\text{-PW}_{10}\text{O}_{36})(t\text{-BuSiOH})_2]$ (**1**) and (b) $(n\text{-Bu}_4\text{N})_3[(\gamma\text{-PW}_{10}\text{O}_{36})(t\text{-BuSiO})_2(\text{SiMe}_2)]$ (**2**).

Table 4. ^{183}W Chemical Shifts and Coupling Constant Connectivity Matrix for $(n\text{-Bu}_4\text{N})_3[(\gamma\text{-PW}_{10}\text{O}_{36})(t\text{-BuSiOH})_2]$ (**1**) and $(n\text{-Bu}_4\text{N})_3[(\gamma\text{-PW}_{10}\text{O}_{36})(t\text{-BuSiO})_2(\text{SiMe}_2)]$ (**2**)

	multiplicity	assignment	W_A	W_B	W_C	$^2J_{WP}$
1	1	W_A	−109.7	*9*	*21.6*	0.6
	2	W_B	*9*	−113.5	21.6	1.1
	2	W_C	*22*	*21.4*	−141.7	1.5
2	1	W_A	−111.9	*8.8*	*21.5*	0.6
	2	W_B	*a*	−113.9	*21.5*	1.2
	2	W_C	*21.5*	*22*	−144.1	1.7

[a] Not observed.

derivatives of trivacant heteropolytungstophosphates, the chemical shifts of **1** and **2** move toward low frequency, as compared with $[\gamma\text{-PW}_{10}\text{O}_{36}]^{7-}$ ($\delta = -12.5$ ppm).[8b] This is in agreement with the IR high-frequency shift, which indicates a rigidification of the whole structure.

^{183}W NMR Spectroscopy. The ^{183}W NMR spectra of **1** and **2** are presented in Figure 4. The chemical shifts and homo- and heteronuclear coupling constants are given in Table 4. For the following discussion, we use a schematic planar representation of the γ-PW_{10} framework (Chart 3) in which edge and corner junctions are symbolized by heavy and dotted lines, respectively.

^{183}W spectra of both compounds are very similar and display three signals of relative intensity 1:2:2, consistent with the retention of the parent polyoxotungstic structure. Thus, in solution polyanions **1** and **2** adopt the symmetric conformation C_{2v}, with three kinds of tungsten atoms which are labeled A, B, and C (Chart 3). All ^{183}W resonances appear as doublets due to coupling with the central phosphorus atom. By ^{31}P decoupling, each signal is reduced to a single line which allows the $^2J_{WW}$ coupling constants to be determined more easily. Assignments of peaks can be done on the basis of relative intensities and homonuclear coupling constants. So, the signal of relative intensity 1 is attributed to both tungsten atoms $W_A(5,6)$ which are located in a plane of symmetry. These atoms belong to a trimetallic unit. They are bonded via a double μ-oxo

Chart 3. Polyhedral and Schematic Planar Representations of the Polytungstic Framework of γ-PW_{10} (C_{2v} Symmetry)

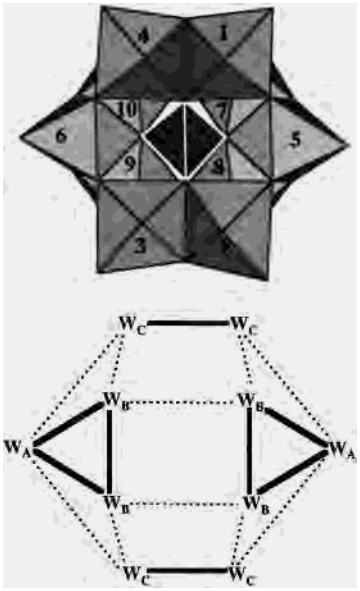

bridge ($^2J_{WW} \approx 9$ Hz, edge-sharing junction) to W_B(7,8 and 9,10) tungsten atoms, and are bonded via a single μ-oxo bridge ($^2J_{WW} \approx 22$ Hz, corner-sharing junction) to W_C(1,2 and 3,4) tungsten atoms. Among both resonances of relative intensity 2, only the high-frequency signal exhibits a small coupling constant ($^2J_{WW} \approx 9$ Hz): it must be assigned to W_B. This signal also has a large coupling constant ($^2J_{WW} \approx 22$ Hz), due to the corner-sharing junction with tungsten atoms W_C. Finally, the low-frequency peak of relative intensity 2 (W_C) exhibits only one pair of satellites in agreement with two corner-sharing junctions between atoms W_B and W_C and W_A and W_C. All coupling constants are consistent with the expected values for a saturated polyoxotungstic structure. In particular, J_{AC} coupling is higher than 20 Hz, whereas in the vacant structure $SiW_{10}O_{36}^{8-}$, this coupling is lower than 10 Hz: this agrees with the fact that terminal oxygen atoms bordering the lacuna of the parent structure become μ-oxo bridging atoms in the organosilyl derivative. As already mentioned, the ^{183}W NMR spectra of both anions are very similar; all resonances of **2** are only slightly shielded with respect to those of **1**. The most affected resonance ($\Delta\delta$ −2.4 ppm) corresponds to the tungsten W_C connected to the *t*-BuSi group (Table 4). This subtle difference could be attributed to the small geometrical modification of the polyoxotungstic framework induced by the addition of the $SiMe_2$ group.

^{29}Si NMR Spectra. ^{29}Si CP-MAS and ^{29}Si solution spectra have been recorded for compounds **1** and **2**. Spectra of both compounds differ by the number of resonances and their chemical shifts. They are represented in Figures 5 and 6.

[(*n*-Bu_4N)$_3$[(γ-$PW_{10}O_{36}$)(*t*-BuSiOH)$_2$]. The solution ^{29}Si NMR spectrum of **1** exhibits a single signal at −44.6 ppm, in accordance with the global C_{2v} symmetry observed in ^{183}W NMR. This signal appears as a multiplet, due to coupling with the nine protons of the *t*-Bu groups ($^2J_{SiH} = 6.7$ Hz) (Figure 5a). In the proton-decoupled spectrum, this peak is reduced to a singlet, with tungsten satellite signals around it ($^2J_{WSi} = 9.5$ Hz). The chemical shift and coupling constant are similar to those observed for the organosilyl derivative [$As^{III}W_9O_{33}$(*t*-BuSiOH)$_3$]$^{3-}$.[7b] From the solution NMR spectra, it appears then that the organosilyl anion [(γ-$PW_{10}O_{36}$)(*t*-BuSiOH)$_2$]$^{3-}$ adopts a more symmetrical conformation (C_{2v}) than in the crystal

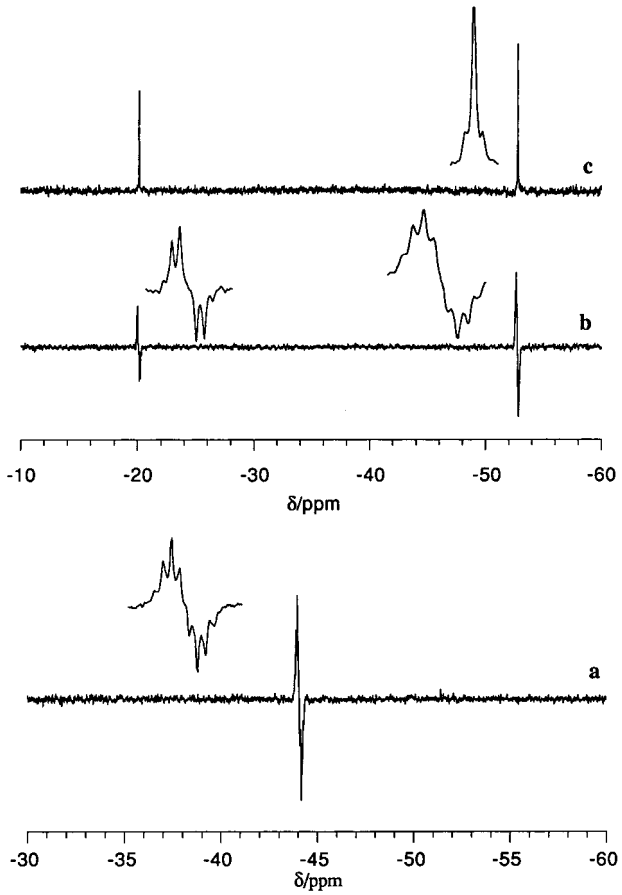

Figure 5. ^{29}Si solution spectra of (*n*-Bu_4N)$_3$[(γ-$PW_{10}O_{36}$)(*t*-BuSiOH)$_2$] (**1**) and (*n*-Bu_4N)$_3$[(γ-$PW_{10}O_{36}$)(*t*-BuSiO)$_2$($SiMe_2$)] (**2**): (a) undecoupled INEPT spectrum of **1**; (b) undecoupled INEPT spectrum of **2**; (c) inverse-gated ^{1}H-decoupled spectrum of **2** with expansion of the low-frequency signal showing the tungsten satellites.

(pseudo-C_s). This could result from a dynamic process in which the two Si−OH units exchange their status (donor or acceptor) in the intramolecular H-bond: thus, through that process the two SiOH groups become equivalent on the NMR time scale. Note that the two OH groups also give rise to a unique proton resonance at 5.0 ppm. Then, it was interesting to search whether this dynamic process could also be observed in solid-state NMR.

The 4 kHz ^{29}Si CP-MAS spectrum of **1** presents two isotropic resonances ($\delta_{iso} = -\sigma_{iso} = -39.0$ and −44.6 ppm), with the same relative integrated intensity, corresponding to two inequivalent Si atoms, in accordance with crystallographic data. At slow rotation speed the MAS spectrum presents the typical pattern with spinning sidebands, which allows the principal values (σ_{11}, σ_{22}, and σ_{33}) of the chemical shift tensor of both ^{29}Si atoms to be determined (Table 5).

These components are defined as follows: $|\sigma_{33} - \sigma_{iso}| \geq |\sigma_{11} - \sigma_{iso}| \geq |\sigma_{22} - \sigma_{iso}|$.

Alternatively the chemical shift tensor can be characterized by σ_{iso}, the shielding anisotropy $\Delta\sigma$, and the asymmetry parameter η:

$$\sigma_{iso} = {}^1/_3(\sigma_{11} + \sigma_{22} + \sigma_{33})$$

$$\Delta\sigma = \sigma_{33} - {}^1/_2(\sigma_{11} + \sigma_{22})$$

$$\eta = (\sigma_{22} - \sigma_{11})/(\sigma_{33} - \sigma_{iso})$$

The low-frequency isotropic signal, which appears at the same position as the single line observed in solution ($\delta_{iso} = -44.6$

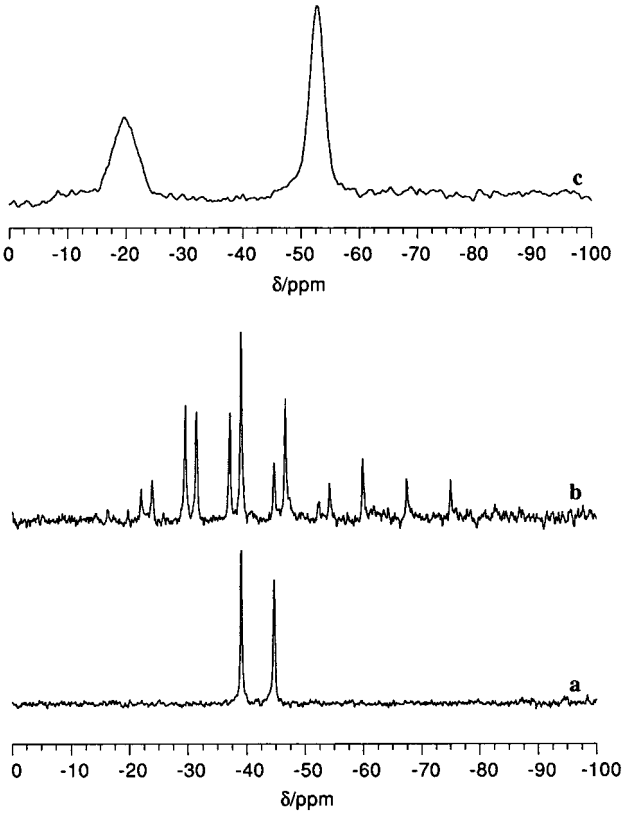

Figure 6. ^{29}Si CP-MAS spectra of $(n\text{-Bu}_4\text{N})_3[(\gamma\text{-PW}_{10}\text{O}_{36})(t\text{-BuSiOH})_2]$ (**1**) and $(n\text{-Bu}_4\text{N})_3[(\gamma\text{-PW}_{10}\text{O}_{36})(t\text{-BuSiO})_2(\text{SiMe}_2)]$ (**2**): (a) **1** at 4 kHz; (b) **1** at 600 Hz; (c) **2** at 4 kHz.

Table 5. ^{29}Si NMR Data for $(n\text{-Bu}_4\text{N})_3[(\gamma\text{-PW}_{10}\text{O}_{36})(t\text{-BuSiOH})_2]$ (**1**) and $(n\text{-Bu}_4\text{N})_3[(\gamma\text{-PW}_{10}\text{O}_{36})(t\text{-BuSiO})_2(\text{SiMe}_2)]$ (**2**)[a]

	solution		CP-MAS			
	Me_2Si	*t*-BuSi	Me_2Si	*t*-BuSi	$\Delta\delta$[b]	η[b]
1		−44.6 (9.5)		−39.0	−27	+0.7
				−44.6	+55	+0.2
2	−20.3	−52.9 (10.5)	−19.6	−52.7	*c*	*c*

[a] δ in parts per million $^2J_{SiW}$ in hertz in parentheses. [b] For the definitions of $\Delta\delta$ and η, see the text. [c] Not determined.

ppm), corresponds to a nearly axially symmetrical tensor ($\eta \approx 0.2$) with a relatively high positive chemical shift anisotropy ($\Delta\sigma \approx 55$ ppm). This compares well with previous determinations on various organosilicon compounds reported by Harris et al.,[23] and with the results obtained by Bonhomme et al., who investigated octameric vinylsilasesquioxane:[24] in the last case, the chemical shift tensor for the vinyl−SiO_3 groups, with approximate C_{3v} symmetry, are characterized by $\eta = 0-0.3$ and $\Delta\sigma \approx 23$ ppm. For the high-frequency resonance of **1** ($\delta_{iso} = -39.0$ ppm), the chemical shift anisotropy amounts to about half the previous value ($\Delta\sigma \approx -27$ ppm), and there is strong deviation of the shielding tensor from axial symmetry ($\eta \approx 0.7$). Accordingly, this signal has to be assigned to Si(2) with a dissymmetrical environment, and the low-frequency signal to Si(1), which presents a nearly axial symmetry.

$(n\text{-Bu}_4\text{N})_3[(\gamma\text{-PW}_{10}\text{O}_{36})(t\text{-BuSiO})_2(\text{SiMe}_2)]$. In solution the ^{29}Si NMR spectrum of **2** shows two signals of relative intensity 1:2. The low-frequency resonance, at −52.9 ppm, is a poorly resolved multiplet, due to the coupling with the nine protons of the *t*-Bu group ($^2J_{SiH} = 6.7$ Hz) (Figure 5b). The other signal, at −20.3 ppm, is a heptet ($^2J_{SiH} = 7.4$ Hz), due to the coupling with six protons. The chemical shift and multiplicity of this signal are characteristic of a $SiMe_2$ unit. In the proton-decoupled spectrum, both resonances become singlets (Figure 5c). The signal at −52.9 ppm, of relative intensity 2, is surrounded by a pair of satellites ($^2J_{WSi} = 10.5$ Hz), attributed to the coupling of silicon atoms of the *t*-BuSi unit with W_C tungsten atoms. The coupling constant, slightly greater than that observed for **1**, suggests an opening of the Si−O−W angle by grafting of a $SiMe_2$ group. Concerning the chemical shifts, the resonance of *t*-Bu is shielded by more than 8 ppm with respect to **1**; a similar behavior was already observed for the capped organosilyl derivatives $[PW_9O_{34}(t\text{-BuSiO})_3(\text{SiR})]^{3-}$ and $[AsW_9O_{33}(t\text{-BuSiO})_3(\text{SiH})]^{3-}$ with respect to the open-structure anions $[PW_9O_{34}(t\text{-BuSiOH})_3]^{3-}$ and $[AsW_9O_{33}(t\text{-BuSiOH})_3]^{3-}$.[7b] In addition, the $SiMe_2$ resonance is strongly shielded with respect to a $SiMe_2$ unit directly grafted on the polyoxometalate framework (i.e., $[PW_9O_{34}(\text{SiMe}_2)_3]^{3-}$).[25]

In the solid state, the 4 kHz ^{29}Si CP-MAS spectrum of **2** presents only two resonances at −19.6 and −52.7 ppm, respectively, in agreement with the chemical shifts observed in solution. Both signals are significantly broader than for **1**; in particular the width of the $SiMe_2$ resonance reaches about 450 Hz (nearly 6 ppm). The resonance of the *t*-BuSi units is slightly more narrow (∼3 ppm) and seems to correspond to a unique isotropic signal. Thus, contrary to **1**, **2** likely adopts in the solid state the same conformation as that in solution, corresponding to a C_{2v} symmetry (Figure 3).

Conclusion

Synthesis of bis(*tert*-butylsilyl)decatungstophosphate $[(\gamma\text{-PW}_{10}\text{O}_{36})(t\text{-BuSiOH})_2]^{3-}$ has been performed by reacting *t*-$BuSiCl_3$ with $[\gamma\text{-PW}_{10}\text{O}_{36}]^{7-}$. X-ray crystallographic investigation reveals an open structure with two unequivalent *t*-BuSi(OH) groups attached to the polyoxometalate backbone through two W−O−Si bridges. The relatively short distance (2.63 Å) between both silanol groups suggests the presence of an intramolecular hydrogen bond, which is however labile in solution.

This anion reacts with methyldichlorosilane to yield a heterosilylated "closed-structure" anion, where the two *t*-BuSi groups become equivalent.

This work demonstrates the versatility of behavior of the divacant γ-anion with respect to organosilyl groups: actually, the four nucleophilic surface oxygen atoms of $[\gamma\text{-PW}_{10}\text{O}_{36}]^{7-}$ or $[\gamma\text{-SiW}_{10}\text{O}_{36}]^{8-}$ are able to bind isolated $[t\text{-BuSiOH}]^{2+}$ groups, μ-oxo-bridged $[(\text{RSi})_2\text{O}]^{4+}$ dimeric units,[26] or more complex siloxane moieties such as the linear heterosilyl [*t*-BuSiO(Me)SiO(*t*-Bu)Si]$^{4+}$ or the tetracyclosiloxane $[(\text{RSiO})_4]^{4+}$ groups.

Supporting Information Available: X-ray crystallographic file for **1** in CIF format. This material is available free of charge via the Internet at http://pubs.acs.org.

IC0004784

(23) Harris, R. K.; Pritchard, T. N.; Smith, E. G. *J. Chem. Soc., Faraday Trans. 1* **1989**, *85*, 1853.
(24) Bonhomme, C.; Tolédano, P.; Maquet, J.; Livage, J.; Bonhomme-Coury, L. *J. Chem. Soc., Dalton Trans.* **1997**, 1617.
(25) Mazeaud, A.; Ammari, N.; Robert, R.; Thouvenot, R. Manuscript in preparation.
(26) Mayer, C. R.; Fournier, I.; Thouvenot, R. *Chem. Eur. J.* **2000**, *6*, 105.